6_Taylor_and_francis_2023.pdf

by Erna Yuliwati

Submission date: 14-Jun-2023 01:53PM (UTC+0700)
Submission ID: 2115786277
File name: 6_Taylor_and_francis_2023.pdf (2.3M)
Word count: 12618
Character count: 70301

11 Mixed Matrix Membrane on Agriculture Industry

E. Yuliwati and S. Martini
Universitas Muhammadiyah Palembang

A.F. Ismail and G. Pei Sean
Universiti Teknologi Malaysia

CONTENTS

DOI: 10.1201/9781003167327-13

11.1 INTRODUCTION

Water is indispensable for every human being, and water usage has been reported to be under great stress due to climate change, urbanization, industrialization, population growth, and food demands. These factors have asserted an extra discussion in the water purification industry. Many conventional and non-conventional technologies namely, adsorption, disinfection, coagulation, and flocculation have been developed to treat water and wastewater to reach the desired water quality for daily use [1]. Few technologies have failed to satisfy the level of water standards. Membrane technology has become the most viable option to overcome this issue [2]. Polymeric and ceramic membrane materials have been used extensively in the water and wastewater treatment field. The increasing awareness of keeping environmental sustainability has resulted in an increasing interest in creating effective membrane systems to purify contaminated water and wastewater. As these contaminated solutions derived from various industrial, household, and agricultural activities contain harmful pollutants giving negative impacts on the environment and human health, proper treatment then is crucial to improve water quality before final disposal [3].

Generally, membrane science research can be divided into seven major areas, that is, material selection, material characterization, membrane fabrication, membrane characterization and evaluation, transport phenomena, membrane module design, and process performance. Among these areas, material selection that is further used for membrane fabrication is the most important part of the membrane technology, and this phenomenon can be reflected by the significant technique [2–4]. Over the years, researchers have improved the performance of membranes [5–7]. They combined the effective features of polymeric and organics additives that are called mixed matrix membranes (MMMs). MMMs are comprising polymer matrix-containing fillers that can be an alternative to overcome the limitations of laminate membranes. MMMs can offer additional functions such as antifouling properties [8], enzyme mobilization [9], mechanical reinforcement, and removal of pollutants in the aqueous phase [10].

Several types of inorganic fillers such as silica [11], zeolite [12], TiO_2 [13,14], carbon nanotubes [15,16], multiwalled carbon nanotubes [17], and silver [18] have been widely used. Figure 11.1 shows various inorganic fillers utilized in preparing MMMs for water purification applications.

MMMs preparation takes days for homogenization that is caused by agglomeration tendency [19]. The incompatibility between inorganic fillers and polymer matrix provokes the formation of undesirable voids in the interface that are difficult to avoid. Meanwhile, MMMs can be defined as membranes that contain homogeneously dispersed fillers with a small composition of nanomaterials. MMMs can be also reused by adjusting pH, contributing to further reduction of harmful wastewater. They can simultaneously remove pollutants from an aqueous solution by adsorption and size exclusion [20,21]. Moreover, MMMs are more suitable for mass production of large-area membranes applicable to standard membrane modules in wastewater filtration.

Incorporating organic polymer with inorganic nanofillers has afforded a viable matrix membrane with overwhelming performance for liquid separation processes

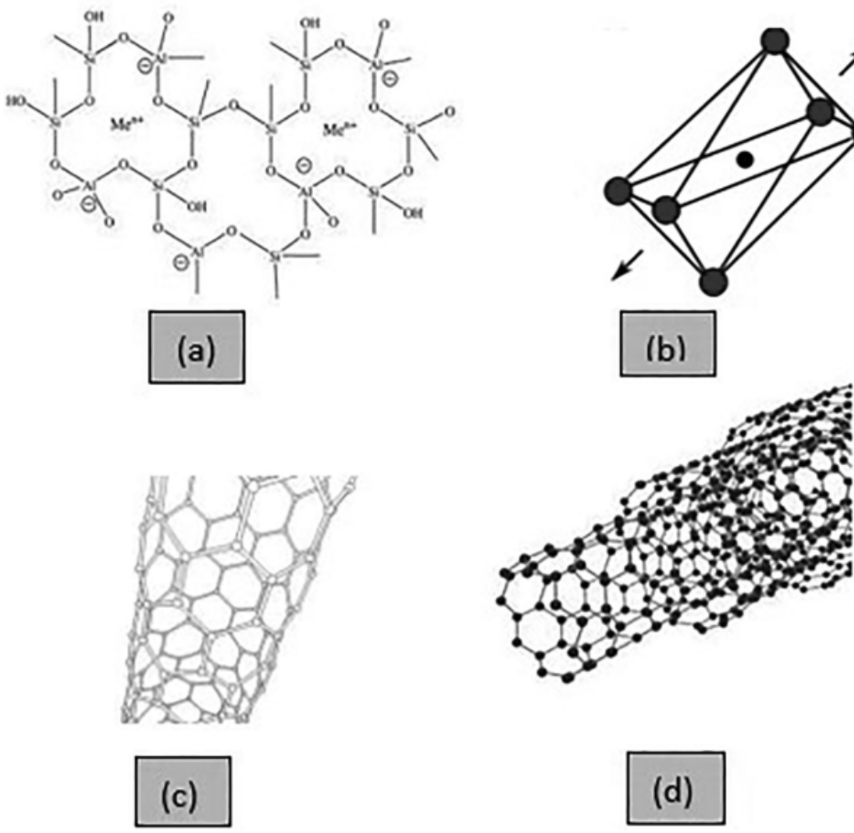

FIGURE 11.1 Various inorganic fillers in preparing MMMS for water purification: (a) zeolite, (b) metal oxide, (c) carbon nanotubes, and (d) multiwalled carbon nanotubes.

on industrial adoption. Table 11.1 summarizes the inorganic fillers for water treatment applications [17–21]. In membrane-based separation technology, Li et al. [19] considered using TiO_2 nanofiller in PA TFC membrane for the water treatment process. Their results revealed that the optimum membrane that contains 5 wt.% TiO_2 gives the better flux and selectivity. Further increase of TiO_2 content led to the significant reaction interference of nanofillers in the PA structure resulting in reduction in salt rejection due to a low degree of polymerization. Others researched zeolites that can be synthesized with SiO_2 higher or lower than in nature for the same framework type. Higher SiO_2 generally gives greater hydrothermal stability, stronger acid catalytic activity, and greater hydrophobicity as adsorbents. Conversely, lower SiO_2 gives greater cation exchange capacity and higher absorbance for polar molecules. Both natural and synthetic forms of the same zeolite are available in commercial quantity. The variable phase purity of the natural zeolite and chemical impurities are costly to remove. Zinc oxide is one of the metal oxides that has received significant attention due to its low cost, high surface area, photocatalytic activity, and

TABLE 11.1
Summary of Inorganic Fillers for Water Treatment Applications

Inorganic fillers	Properties	References
Iron-based	Highly reactive, larger surface area, detoxification of organic and inorganic pollutants, adsorption capacity, hydrophilic, fouling resistant, magnetic oscillation, hydraulic turbulence.	23, 26, 57
Silver-based	Anti bacterials, good transport facilitator, good selective barrier, high reactivity, low toxicity to humans	23, 24, 57, 59
Zeolite	Hydrophilic, fouling resistant, anti-adhesion to protein, effective sorbents, ion exchange media for metal ions	38, 39
Silica-based	Hydrophilic, fouling resistant, anti-adhesion to protein	18, 19
Titanium dioxide-based	Hydrophilic, fouling resistant, anti-adhesion to protein, photo catalytic, disinfection, anti-adhesion to protein, decomposition of organic compounds, reduced surface roughness, oxidative and reductive catalyst for organic and inorganic pollutant, killing bacteria.	10, 25, 30, 42
Carbon nanotube-based	Anti-microbial, hydrophilic, biofouling resistant, anti-adhesion to protein, selective sorbents for organic compound.	15, 16, 27, 28, 29

antibacteria properties [22]. Wang et al. [23] improved cellulose acetate membranes using Zeno-NPs (4 wt.%) which led to the enhancement of 111.1% of the flux compared to the pristine membranes. Previous researchers have found that the improvement in membrane permeability occurred due to the presence of zinc oxide (ZnO) in the PES membrane [24]. Additionally, this membrane has the highest fouling resistance during oleic acid filtration. However, at high polymer concentration, the mixed matrix membrane shows a reduction in the membrane permeability due to a drop in the dispersion rate. Silica nanofillers have also rapidly become focus of research on mixed matrix membranes due to their unique characteristics such as small size, strong surface energy, high scattered performance, and thermal resistance. Moreover, silica nanofiller has wider resources and lower price than that of TiO_2 nanofiller [25].

Zeolite has the chemical formula, $Mn_2OAl_2O_3.xSiO_2.yH_2O$, where the charge-balancing non-framework cation M has valence n, while x is 2.0 or more, and y is the moles of water in the voids. The Al and Si tetrahedral atoms in the forms of AlO_4 and SiO_4 tetrahedra are linked by shared oxygen ions. Synthetic zeolite can be more attractive for specific applications. Yellowtail et al. synthesized a nanocomposite membrane by blending zeolite in the polysulfide polymer, resulting in a membrane of better permeability and antifouling ability [25]. The result showed that zeolite raised the water flux up to 1.6 times. This resulted in permeation was attributed to increased hydrophilicity of nanocomposite. The zeolite also provided huge surface energy, which clustered small water molecules producing more polysulfone membrane. Table 11.1 tabulated the summary of inorganic fillers for water treatment applications [26]. The application of MMMs of adding inorganic zeolite in separation and purification processes was used to exclude molecules that are too large to enter the pores and admit smaller ones.

Carbon nanotubes (CNTs) have exceptional properties such as high mechanical and chemical stability and high electrical conductivity [16,27]. The properties of CNTs have made them attractive candidates for overcoming water scarcity and water pollution issues. Several authors have shown that the effect of CNTs in membrane polymer tends to enhance the hydrophilicity due to the decrease in contact angle, leading to greater water flux. The synthesis of polymer/CNT further improves membrane performances with respect to permeability, chlorine tolerance, thermal resistance, solvent stability, and fouling resistance [28] and the method for incorporating CNT to the mixed matrix membrane as in Figure 11.2.

Several authors demonstrate the functionalization of CNTs in a strong acid mixture as illustrated in Figure 11.3 [28]. They observed peaks of 1,680, 1,715, 2,875,

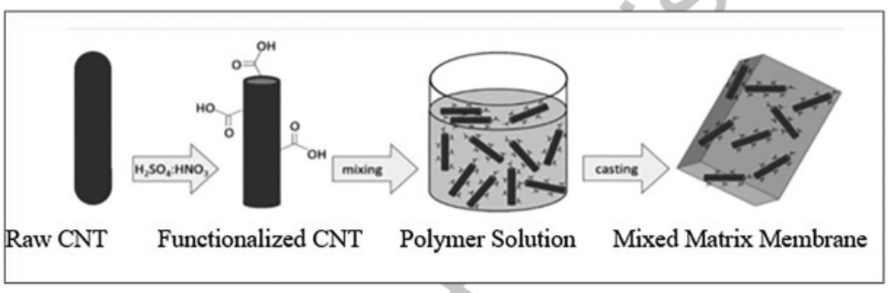

FIGURE 11.2 Schematic representation of MMMs with CNT-fillers.

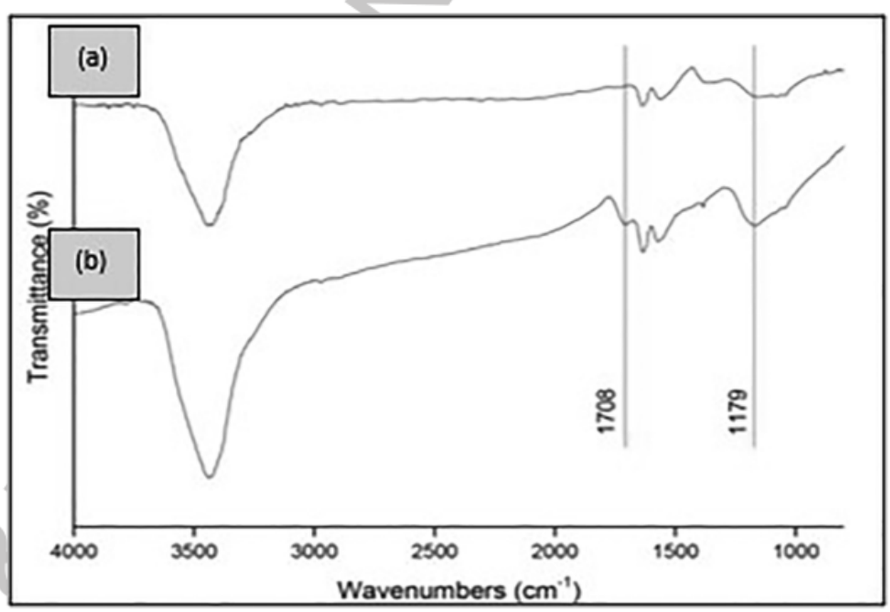

FIGURE 11.3 Functionalization of CNTs: (a) raw CNTs and (b) functionalized CNTs.

and 3,435 cm^{-1} that correspond to COOH, C–C, C–O, C=O, C–H, and –COOH, respectively, with Fourier Transform Infra-Red (FTIR) analysis. The length of CNTs was tens of micrometers before H_2SO_4:HNO_3 treatment, but reduced to hundreds of nanometers after H_2SO_4:HNO_3 treatment [28]. CNTs were broken into smaller CNTs, tips were open, and carboxylic groups were at the tips and defect sites of the CNTs. These results verify the successful functionalization of the CNTs.

The incorporation of multiwalled carbon nanotubes (MWCNTs) throughout the super selective thin-film layer was also explored as a facile approach to producing superior hydrophilic membrane. The unique molecular architecture of the tubes embedding in the membrane matrix has the potential to increase both permeability and selectivity. MWCNTs were not well dispersed in the non-polar solvent of the organic phase, but generally agreed that the rapid transport rates exist because the walls of nanotubes are much smoother (on atomic scales) than other materials leading to the increase in surface area of MMMs. This phenomenon tends to increase the rejection rate of MMMs [29].

11.2 MIXED MATRIX MEMBRANES

The combination of polymeric and inorganic/organic materials in one new material is called mixed matrix membranes (MMMs). MMMs can also be defined as incorporation of nanomaterials in solid–liquid phase or both that are dispersed or embedded in a continuous phase. These phases have been combined to have the effective features of both polymeric and filler. The sole purpose of developing this new material has been to associate the advantageous characteristics of two types of membranes boosting the overall process. Material advancement in membrane technology has made it possible to fine-tune the process efficiency and has successfully paved the way for MMMs in water treatment applications [29].

Figure 11.4 shows the schematic of an ideal MMMs that could offer the physicochemical stability of inorganic/organic material and polymeric materials while promising the desired morphology with higher values of permeate selectivity, hydrophilicity, fouling resistance, along with better thermal, mechanical, and chemical strength over a wider range of temperature and pH [28,29]. Polymer matrix plays a big role in permeability whereas the inorganic filler is a controlling factor for the

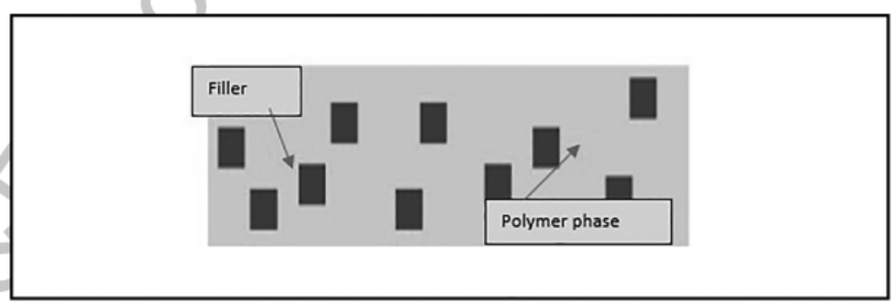

FIGURE 11.4 Schematic of ideal mixed matrix membranes.

selectivity of separation performance. The interfacial compatibility between the two phases is important to serve the desired purpose for such membranes [26]. The addition of fillers asserts their effect on the morphology of MMMs. The transport phenomenon determines the overall performance of newly developed membranes. The interfacial void formation, aggregation, and pore blockage are some of the key effects in resultant MMMs [29]. The presence of interfacial voids creates additional channels that allow the solvent to pass through the membranes [30]. Meanwhile, the mechanical strength and rejection rate are concerned by density. These features should be controlled or avoided by optimizing the process parameters of polymer concentration, filler concentration, casting technique, and coating technique [31–33]. Therefore, addition of these fillers in membrane synthesis could be challenging since controlling the placement of dispersion and its shedding/loss during the process is an important task that restricts its commercialization.

Goh and Ismail summarized their types of MMMs in four different types, namely conventional nanocomposite, thin-film composite with nano thin film, nanocomposite, thin-film composite with nanocomposite substrate, and surface-located nano composite [34]. These types of MMMs based on their corresponding filler types, such as inorganic filler-based MMMs, organic filler-based MMMs, biofilter-based MMMs, and hybrid filler-based MMMs.

11.2.1 Inorganic Filler-Based MMMs

An inorganic filler-based membrane is an active MMM in which inorganic fillers attach themselves to support materials by covalent bonds, van der Waals forces, or hydrogen bonds. These inorganic fillers are prepared through processes such as sol–gel, inert gas condensation, pulsed laser ablation, spark discharge generation, ion sputtering, spray pyrolysis, photothermal synthesis, flame synthesis, low-temperature reactive synthesis, mechanical alloying, milling, and electrodeposition [35].

11.2.1.1 Zeolite Filler-Based MMMs

Recently, many reports demonstrated catalytic activity of polymer–zeolite MMM because the interaction of materials in the membrane matrix and the shape-selective catalytic properties of zeolites can improve permselective separations. The membrane also functions as a separator in the gas phase between different gaseous molecules. Thus, the membrane should be permeable enough to give efficient separation. For liquid-phase separation, metal-organic complexes and inorganic filler such as zeolite have been used [36]. It is well presented mostly that polydimethylsiloxane (PDMS) is incorporated as a polymer matrix because of its high permeability, an affinity for reagents, thermal, mechanical, and chemical stability [37]. Langhendries and Baron studied the catalytic activity of zeolite-filled poly(dimethylsiloxane) polymer membranes [38]. Catalyst performance was found to improve significantly as zeolite-encaged iron-phthalocyanine was incorporated into a dense hydrophobic polymer membrane.

SEM image of a zeolite MMMs showed a homogenous distribution of zeolite particles in the polymer matrix at different loads [35,39] (Figure 11.5). Zeolite mixed matrix membranes (zeolite MMMs) are used for sustainable engineering

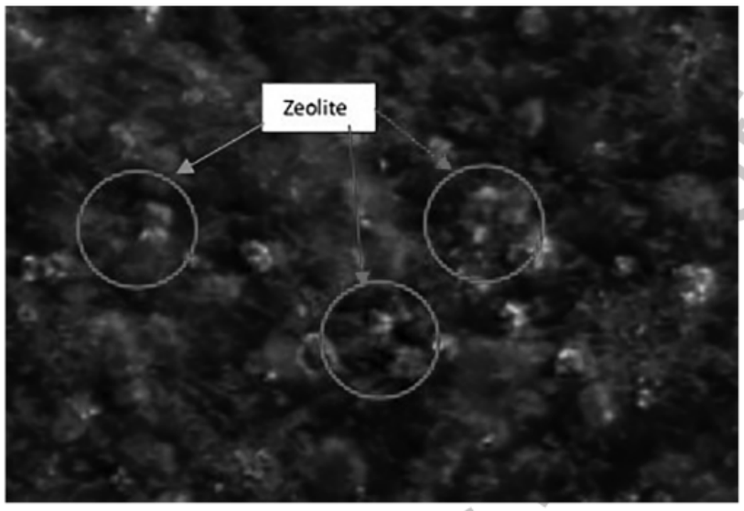

FIGURE 11.5 SEM images of zeolite MMMs.

improvement in catalyst performance. Both mathematical model and kinetics determined exact concentrations in polymer and catalyst, and subsequently, the resulting catalyst activity and selectivity. Their results also indicate that hydrophobic poly-(dimethylsiloxane) is an attractive polymer for the incorporation of the hydrophilic zeolite-encaged iron-phthalocyanine catalyst. As a result, diffusion through composite catalytic membranes can be predicted using the mass transfer coefficients of pure zeolite and pure polymer material, and a tortuosity factor based on the zeolite loading as a catalyst.

Figure 11.5 shows the dispersion of zeolite that is produced by synthesis of MMMs with homogenous mixing between polymer and zeolite. Meanwhile, Drioli and Giorno investigated the incorporation of polydimethylsiloxane (PDMS) into a polymer matrix and silicate for the permeation of various gases [40]. In their study, only a couple of very high-zeolite loadings were investigated, and they indicated that zeolite plays an important role as a molecular sieve in the membrane by facilitating the permeation of smaller molecules while it prevents the permeation of larger ones.

11.2.1.2 Titanium Dioxide Filler-Based MMMs

Titanium dioxide (TiO_2) nanofiller has a high specific area and hydrophilicity that affect the mass transfer during the membrane process. At lower TiO_2 concentration (< 2 wt.% of TiO_2), an increase in the amount of hydrophilic TiO_2 tends to draw more water into polymer dope, resulting in an increase in the length of finger-like macrovoids and a decrease in the thickness of the intermediate sponge-like layer [41]. Whereas at higher concentrations of the TiO_2 (3–10 wt.% of TiO_2), an increase in TiO_2 concentration would increase the viscosity of the polymer dope and decrease the rate of water intrusion into polymer dope. This phenomenon then results in shorter finger-like macrovoids and a thicker intermediate sponge-like layer.

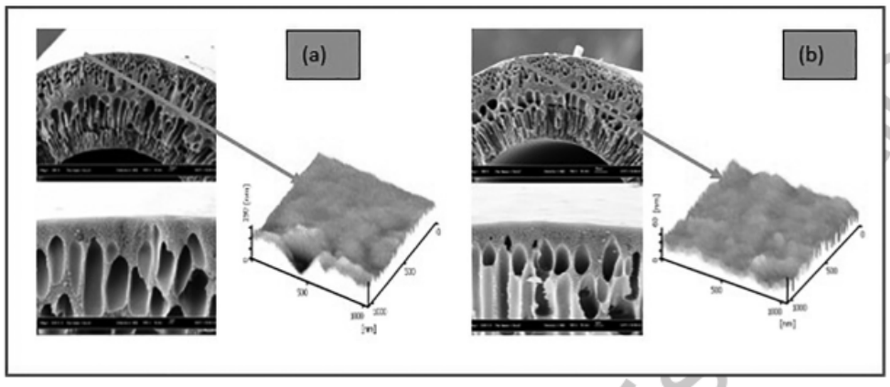

FIGURE 11.6 (a) FESEM images of cross section and AFM images of the outer surface of MMMs with (a) lower TiO_2 and (b) higher TiO_2 concentrations.

A field emission scanning electron microscope (JEOL JSM-6700F) was used to examine the morphology of the PVDF hollow fiber membrane. Prior to analysis, the membrane samples were first immersed in liquid nitrogen and fractured carefully [42]. The samples were then coated with sputtering platinum before testing. The FESEM micrographs of the cross section and outer surface of the hollow fiber membranes were taken at various magnifications.

Figure 11.6 illustrates the AFM image of membrane surface that is not smooth. The nodule-like structure and nodule aggregates are formed at PVDF/TiO_2 MMMs' surface. Yuliwati et al. [42] reported the effect of TiO_2 on MMMs surface. They reported that the surface became smoother, and the nodules were separated from each other leading to a rougher MMMs surface than that of a neat PVDF membrane. This result may be attributed to PVDF/TiO_2 MMMs outer surfaces that experienced coalescence and orientation of polymer aggregates before gelatin in the external coagulation contained. The relaxation of the polymer occurs on the outer surfaces during relaxation, and the macromolecules tend to coil and entangle with each other, enhancing the fusion of nodular aggregates.

11.2.1.3 Carbon Nanotubes Filler-Based MMMs

Carbon nanotubes (CNTs) often refer to single-wall carbon nanotubes (SWCNTs) with diameters in the range of a nanometer. CNTs exhibit remarkable electrical conductivity, while others are semiconductors. They have exceptional tensile strength and thermal conductivity due to their nano structure and the strength of the bonds between carbon atoms. These properties are expected to be valuable in many areas of technology, such as electronics, optics, mixed matrix materials, and nanotechnology. Carbon nanotube membranes can be classified into different categories according to the fabrication methods; however, the two broad classes are: (a) freestanding CNT membranes, and (b) mixed (nanocomposite) CNT membranes. The two main types of freestanding CNT membranes, typically used in desalination and water treatment applications, are vertically aligned CNT (VACNT) membranes and bucky-paper membranes [43].

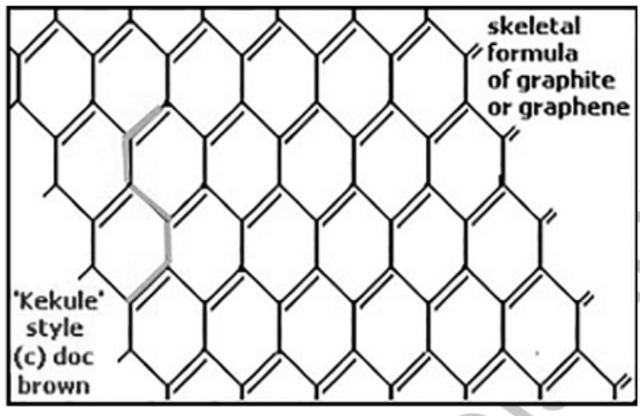

FIGURE 11.7 Structure molecule of carbon nanotubes (CNTs)-based membranes.

Figure 11.7 shows the zigzag and armchair configurations that are part of some structures of a single-walled nanotube. On some carbon nanotubes, there is a closed zigzag path that goes around the tube. The length of the carbon–carbon bonds is fairly fixed. There are constraints on the diameter of the cylinder and the arrangement of the atoms on it.

CNTs are the most used fillers in the development of MMMs. To employ CNTs as effective reinforcement in the polymeric matrix, proper dispersion, and suitable interfacial adhesion between CNTs and the polymer matrix have to be guaranteed. Figure 11.8 shows the application of CNTs in many industries, such as energy, biology, electronics, materials, agriculture, and tools. The current trend in polymeric MMMs is the incorporation of filler-like nanoparticles to improve the separation performance. Ismail et al. fabricated carbon nanotubes-mixed matrix membranes (CNT-MMMs) that offer a viable route to overcome the limitation demonstrated by the conventional polymeric and inorganics membranes. The excellent diffusivity properties of CNT have a promising outlook in wastewater separation processes.

11.2.2 Organic Filler-Based MMMs

Organic filler-based membranes are a modern type of MMMs in which organic fillers (such as cyclodextrin, polypyrrole, polyaniline (PANI), chitosan beads, wheat straw, yellow birch, pine, and rice husk) are introduced into substrate matrix, mostly through blending and phase inversion [44]. Organic fillers have the distinct advantage of having more functional groups attached to them, hence making them more adaptable than inorganic fillers. Their ability to attach themselves to a substrate through chemical reactions or binding themselves, especially with a hydrophobic surface makes them a better option for developing specialized (antifouling, highly hydrophilic, specific component rejection or higher porosity) membranes [45]. Zhao et al. synthesized a nanocomposite membrane by blending PANI nanofibers in polysulfone polymer, resulting in a membrane having better permeability and antifouling properties [46]. As a result, the water flux of PANI nanofibers increased up to 1.6

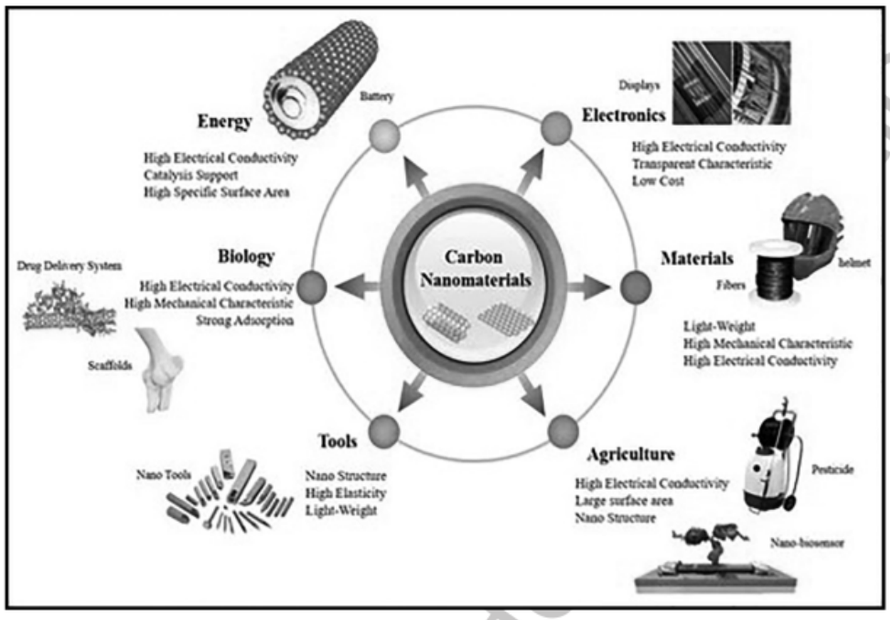

FIGURE 11.8 The applications of carbon nanotubes (CNTs) [28].

times. This improvement can be attributed to the increasing hydrophilicity of nanocomposite, since PANI (molecular structure as in Figure 11.9) fibers provided huge surface energy, which clustered the small water molecules, hence producing a more permeable polysulfone membrane .

Teli et al. also obtained the same results for PANI-based nanocomposite membranes with added polyvinylpyrrolidone (PVP) [47]. They successfully enhanced the pure water flux, antifouling, separation efficiency, and mechanical strength of the resultant membranes with further PVP additions. Their study showed satisfying results because the addition of PVP (below 0.5 wt.%) with PANI organic filler in polysulfone matrix produced the aforementioned characteristics in the resulting membrane. BSA rejection through these membranes only occurs due to the hydrophilic nature of nanofillers (PANI) on the surface and the sieving mechanism due to the larger sizes of BSA molecules, though the addition of PVP may not affect the rejection significantly [47]. Zhong et al. blended a β-cyclodextrin polyurethane into a polysulfone matrix for removing Cd^{+2} ions from water [48]. The addition of β-cyclodextrin polyurethane increased the permeability of the MMM to 489 $Lm^2.h^{-1}$ by providing more wide pores on the surface, higher hydrophilicity, and better connectivity within finger-like pores.

11.2.3 Biomaterials-Based MMMs

Incorporation of biomaterials (biofillers) (such as aquaporin, amphiphilic, or lignin) into continuous matrix is an innovative technique to enhance the effectiveness of membrane technology. Biofiller-based MMMs deliver better permeability,

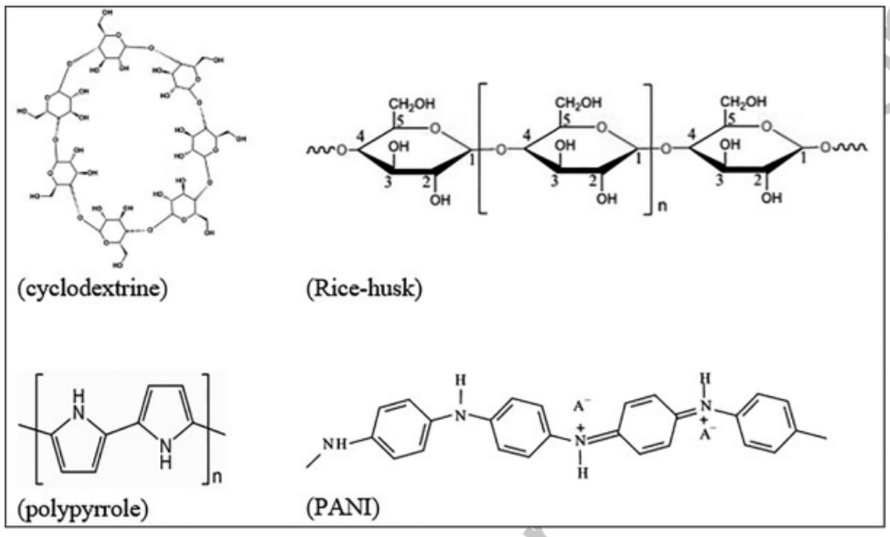

FIGURE 11.9 Various types of organic fillers.

antifouling ability, and certain functionalities such as mechanical reinforcement effect, which are either lacking or quantitatively low in the nascent membrane [49]. Two design strategies to synthesize these membranes are extensively reported in the literature. In the first strategy, aquaporin containing lipid bilayer is coated directly on the membrane substrate, while in the second strategy, vesicles or proteoliposomes (aquaporin incorporated in liposomes/ polysomes) are coated on the support surface [50].

Figure 11.10 presents a design of a vesicular membrane incorporated with a commonly used biofiller, such as aquaporin. Recent work by Wang et al. proposed that the introduction of aquaporin filler in amphiphilic triblock polymer vesicles (PMOXA15-PDMS10-PMOXA15) demonstrated an excellent performance related to permeability and driving force that was claimed to be 800-fold better than the simple polymeric membranes [51]. These newly developed MMMs also offered the unique ability to achieve a controlled permeability. They were found to be an excellent barrier toward urea, glucose, glycerol, and salt by reporting their relative reflection coefficient higher than unity. Nevertheless, the limiting concentration and incorporation method of biofillers in a polymer matrix have to be accounted properly since they could cause a significant decrease in membrane productivity under different biofiller concentrations [52].

Furthermore, Wang et al. used plant waste as biofiller in their study for cationic dye removal [53]. They added biofiller, e.g., banana peel, tea waste, and shaddock peel in polyethersulfone and reported the rejection of up to 95% of cationic dyes. The addition of such biofillers provided better charge interaction, hydrophobic interaction, and hydrogen bonding, hence improving the overall rejection of developed MMMs. Further improvement in cationic dye removal from wastewater is also suggested if the simple polymeric matrix is removed with biopolymers [53]. Other

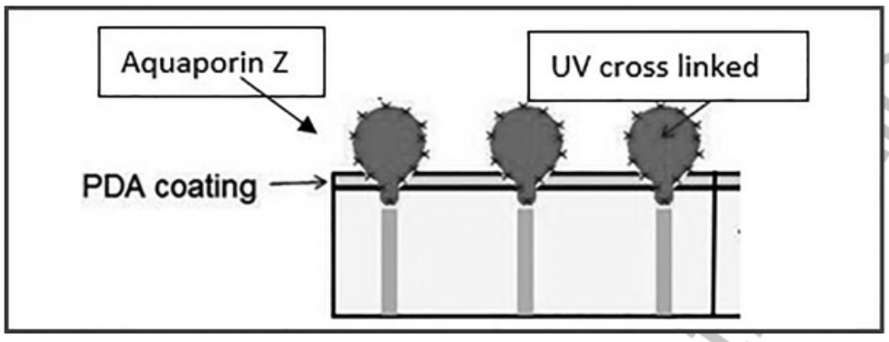

FIGURE 11.10 Design of biofiller mixed matrix membranes.

polymers have also been tested in various studies as Li et al. introduced aquaporin containing liposomes into polyamide imide (PAI) polymer matrix to synthesize a nanofiltration membrane with high permeability and higher rejection efficiency [54]. Their study reveals that at optimal composition (liquid-to-protein ratio of 200), the membrane showed the maximum pure water flux of 36.6 L $m^{-2}h^{-1}$, whereas the rejection of divalent salts was as high as 95%. The high permeability of the membrane was attributed to the availability of more passage for water molecules provided by aquaporin. On the other hand, high rejection of membrane was the direct result of the liposomes selective layer. Nevertheless, the method of incorporation of aquaporin in any matrix needs proper consideration since aquaporin placed near the top surface or exposed to the external environment would lose its activity.

Nevárez et al. synthesized gold and silver nanoparticles for producing a composite membrane for metal ions rejection [55]. They incorporated three different types of propinated lignin (kraft) in cellulose triacetate (CTA) through vapor-induced phase separation method. These showed that propinated kraft lignin (KL) improved the mechanical strength of the resultant KL/CTA membrane. Propination of kraft lignin increased the compatibility of the propyl group with cellulose acetate due to more London dispersion forces between the biofiller and the substrate polymer. However, propination adversely affected the mechanical characteristics of the developed membranes in the cases of organoslov (OL) and hydrolytic (HL) lignin. Propination in OL and HL lignin increased the particle sizes of resultant biofillers that diminished the adhesion between CTA and incorporated lignin nanoparticles, thus making the membranes less mechanically stable. Rejection measure for propinate Kl/OL/HL-based CTA MMMs showed a better rejection rate of arsenic ions for OL-based CTA MMMs (17%–22.8%), while the other two lignin suffered reduction due to antagonistic effects of divalent ions in the solution [56].

11.2.4 Hybrid Filler-Based MMMs

Hybrid fillers are a recent addition to the MMMs technology. This type of membrane contains two different fillers (independently or in composite form) added to the continuous phase. These hybrid materials are incorporated either to accomplish

any targeted purposes or to improve the overall process effectiveness of the resultant membrane. A conceptual multifunctional membrane is depicted with hierarchal nanofillers where, on different layers, different types of nanofillers are introduced to achieve diverse functionalities. Mahmoudi et al. introduced the combination of iron (II, III) oxide and polyaniline into a polyethersulfone matrix to be able to accomplish 85% of Cu (II) removal from water [57]. The results showed that adsorption, in this case, was the dominating separation mode, otherwise this membrane could offer better reusability and durability.

A novel hybrid material chitosan-montmorillonite (CS-MMT) was dispersed in a polyethersulfone (PES) matrix by Saf et al. [58]. This novel hybrid filler CS-MMT raised the membrane antifouling ability due to its highly hydrophilic nature and increased the membrane mechanical strength by restricting the polymer chain mobility forming interrelated structures. They showed that a high flux recovery of up to 92% was achieved due to a loose active layer and the enhanced hydrophilic nature of the membrane [59]. Alpatova et al. also synthesized an antifouling MMM through inclusion of Fe_2O_3 nanoparticles and multiwalled carbon nanotube (MWCNT) in polyvinyldene fluoride (PVDF) [60]. The addition of this hybrid filler raised the degradation of fouling compounds such as cyclohexanoic acid and humic acid resulting in better antifouling behavior than that of the nascent one.

11.3 APPLICATION OF MMMS

Membrane-based technologies used for water and wastewater filtration can be a promising alternative to treat wastewater or water including both conventional and emerging pollutants and economic advantages over other water treatment processes. As aforementioned, MMMs comprising polymer matrix-containing fillers can be a viable alternative to overcome the limitation of laminate membranes. Only a small amount of inorganic nanomaterials is required to prepare MMMs as compared to the total weight, thereby minimizing the environmental and safety issues accompanied by the preparation of inorganic nanomaterials. MMMs can be reused by adjusting pH and simultaneously removing different types of pollutants from aqueous solution by adsorption and size exclusion. Moreover, MMMs are more suitable for mass production of large-area membranes used in water and wastewater treatment. In this chapter, we review the MMMs application in the agriculture industry, such as the polyvynilidene fluoride/titanium dioxide for virgin coconut oil purification and polysulfone/titanium dioxide fillers for palm oil wastewater.

11.3.1 MMMs on Purification of Virgin Coconut Oil

Virgin coconut oil (VCO) is obtained from the fresh and mature kernel (12 months old from pollination) of the coconut (Cocos nucifera L.) by mechanical or natural means with or without the application of heat, which does not lead to alteration of the nature of oil. VCO has not undergone chemical refining, bleaching, or deodorizing. VCO consists mainly of medium-chain triglycerides, which are resistant to peroxidation. VCO has been also acknowledged as the healthiest crop oil and can be extensively used in various fields such as food, beverage, medicinal, pharmaceutical,

TABLE 11.2
Essential Composition and Quality Factors of Virgin Coconut Oil (SNI 7381:2008)

Parameter	Standard, SNI
Moisture and impurities (%)	Max 0.1
Volatile matters at 120°C (%)	Max 0.2
Free Fatty Acid (%)	Max 0.2
Peroxide Value meq/kg	Max 3
Relative density	0.915–0.920
Refractive Index at 40°C	1.4480–1.4492
Insoluble impurities per cent by mass	Max 0.05
Saponification value (Mg KOH/g oil)	250–260 min
Color	Water clear
Odor and Taste	Natural fresh coconut scent, free of sediment, free from rancid odor and taste

nutraceutical, and cosmetics [61]. VCO is colorless, but multiple processes could change the color of VCO to bright yellow. This color change tends to decrease the VCO quality. The essential composition and quality factors of VCO have been tabulated in Table 11.2 [62].

High-quality VCO has some advantages such as it is odorless, colorless, and free of sediments. The odorless VCO can be produced by filtration through PVDF MMMs, which have porous fibers consisting mostly of titanium elements that are distributed on the MMMs' outer surface. Being covalently bonded and having a very large surface area were influenced by titanium dioxide fillers in PVDF polymer [40,61].

11.3.1.1 Characteristics and Quality of VCO

11.3.1.1.1 Dye Removal

Dyes are colored substances that establish chemical bonds with the substrates. It has been estimated that virgin coconut oil contains dyes contributing to the quality of VCO. The quality of VCO in Indonesia is standardized accordingly (SNI 7381:2008) [62].

11.3.1.1.2 VCO Analysis

The relative density of VCO samples was measured according to the AOAC method (AOAC, 2000) at a temperature of 30°C. The fatty acid profile of VCO samples was measured as fatty acid methyl esters (FAMEs). Prepared FAMEs were injected into the gas chromatography (Shimadzu, Kyoto, Japan) equipped with the flame ionization detector (FID) at a split ratio of 1:20. A fused silica capillary column (0.25 mm), coated with bonded polyglycol liquid phase, was used to analyze the fatty acids. The analytical conditions were an injection port temperature of 250°C and a detector temperature of 270°C. The oven temperature was set up within the range of 170°C–225°C at a rate of 1°C min^{-1} (no initial or final hold). The retention time of FAME standards was used to identify chromatographic peaks of the samples. Fatty

acid content was calculated based on the peak ratio and expressed as g fatty acid/100 g oil. The acid value of all VCO samples was measured by the AOCS method (AOCS, 2009), and FFA was analyzed by the following equation using the conversion factor of 2.81 for lauric acid. The results showed the characteristics of MMMs (PVDF/TiO_2 membrane) that identified four parameters namely odor, color, relative density, and free fatty acid content. Table 11.3 illustrates the composition of VCO after filtration.

11.3.1.2 Effect of Surface Morphology on Filtration of PVDF/TiO_2 MMMs

The results of the surface morphological analysis of the MMMs were obtained using a scanning electron microscope (SEM) as shown in Figure 11.11. The figure shows the surface morphology of bio-adsorbent obtained using an electron microscope scanning the field emission with magnification 374 times for each samples a and b. Figure 11.11a and b illustrates bio-adsorbent used by SEM with magnification of 8,740 and 8,750. The bio-adsorbent pores are spread evenly on the surface area.

The pore diameter can also be measured using the same tool, which is an average of 1.59 µm, as shown in Figure 11.11. The filtration process occurred when the VCO passed through the pores of PVDF/TiO_2 MMMs. The average pore diameter of the PVDF/TiO_2 can be analyzed through SEM. The density of permeate was analyzed

TABLE 11.3
Composition of Produced Virgin Coconut Oil After Filtration

Component	Unit	Total	Standard, SNI [62]
Odor	None	1	1–2
Color	None	1	1–2
Relative Density	gr/mL	0.917	0.915–0.917
Free Fatty Acid	%	0.057	0.03–0.09

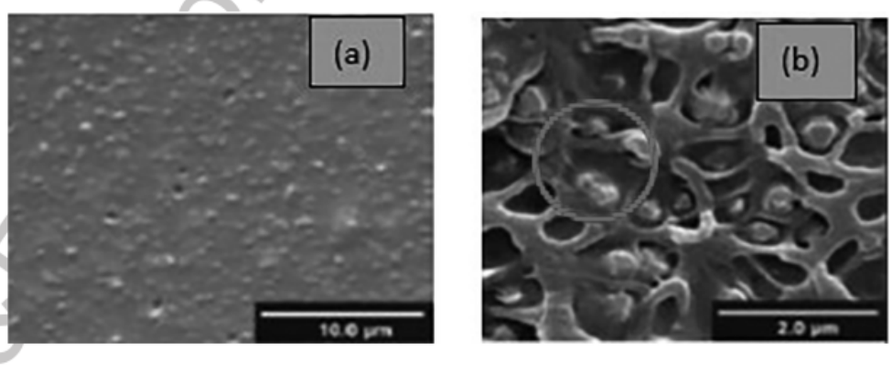

FIGURE 11.11 Surface morphology of MMMs using SEM (a) before and (b) after purification.

by a pycnometer with an average density of 0.917 gr mL^{-1}, free fatty acids (ALB) of 0.057%, as shown in Table 11.4. As can be seen, the MMMs which have a high total porosity and average pore size tend to increase the flux and remove more impurities significantly.

11.3.2 Application of Optimum Process Condition of PVDF/TiO_2 MMMs on Filtration of Palm Oil Wastewater

Wastewater streams typically contain many regulated inorganic and organic contaminants that can restrict their use or disposal thereof. Standards promulgated by state agency that regulate the maximum content of contaminants in wastewater streams disposed into publicly owned treatment works or discharged into waste injection wells have become increasingly stricter. Thus, processes for reducing the content of the inorganic and organic contaminants to an acceptable level in the wastewater streams have been employed to comply with these standards.

Palm oil is broadly produced in Indonesia and its production reached 48.68 million tons in 2018 [63]. Indonesians commonly choose palm oil as an alternative to other vegetable oils for daily needs. The current market showed a high demand of the palm oil industry leading to a higher production rate [64]. Meanwhile, the increase in palm oil production resulted in contaminants in its production wastes, such as solid waste and liquid waste. The contamination of water supplies by traces of the palm oil industry is a global issue causing environmental and health concerns resulting in an increasing demand for water remediation technologies. Nowadays, membrane system has grown up significantly and has received big attention from both academic and industry for answering the problems of water remediation technology. The usage of low-pressure membrane processes such as ultrafiltration has been increasing significantly for water and wastewater reclamation. The properties of wastewater also have a major impact on membrane fouling. Fouling is a major limitation for their implementation and also can affect the permeate quality and overall operation cost.

The palm oil industry mostly generates two types of waste, namely solid and liquid wastes. Liquid waste has been known as palm oil mill effluent, which is thick brownies viscous liquid waste, slurry, has high colloidal suspension, and has an unpleasant odor [65]. POME contains 95%–96% water, 0.6%–0.7% oil, and 4%–5% total solids including 2%–4% suspended solids [9,14]. Suspended solids consist mainly of debris from palm fruit mesocarp. POME was produced from sterilizer condensate, clarification condensate, and hydro-cyclone waste in the amount of 1,130L of each ton of processed palm oil [64]. POME is a non-toxic liquid waste with an unpleasant odor and a high concentration of chemical oxygen demand (COD) and biological oxygen demand (BOD). This composition causes serious pollution and environmental problem to the water sources. Table 11.4 tabulates characteristic of POME and standard discharge of treated POME in Indonesia [65].

Palm oil mill effluent management treatment mostly applied conventional biological treatments of anaerobic or facultative digestion. The aerobic and facultative ponds rely on bacteria to break down the organic matter into simple end products of methane, carbon dioxide, hydrogen sulfide, and water [63,66]. It consists of a series

TABLE 11.4
The Standard Discharge of Treated POME

Parameters	Type of POME	Standard discharge, mg/L	Concentration of pollution loading, mg/L
BOD_5	25,000–29,000	100	225 (1.01)
COD	51,000–64,000	350	888 (0.25)
TSS	18,000–23,000	250	263 (1.02)
Oil and grease	6,000–7,000	25	63 (0.08)
Total nitrogen	750–1,200	50	21.5 (0.53)
pH	4..5	6–9	

of ponds connected to each other where each pond has its own purpose tending to increase the operational cost. Moreover, biological treatment can also produce biogas which is known as a corrosive and hazardous substance. These problems could be overcome by applying a membrane system. It could also treat POME with better consistency regardless of effluent variations allowing recycle process of the selected waste stream within a plant, so treated wastewater could be reused in the mill. The primary advantage of the membrane system is that it lowers the overall cost regarding supply of water and its further treatment namely, the elimination of the pollutant of POME. Moreover, the operational cost of the membrane system is less than conventional treatment. The increase of air gap length in membrane spinning affects the decrease of pure water permeation and wall thickness, the increase of pore size of outer surface skin layer thickness. TiO_2 particles loading possessed smaller pore size, and more apertures inside the membrane that increased the membrane hydrophilicity. Moreover, TiO_2 could degrade the color pigment contained in POME [66]. Some previous studies reported that permeate volume is enhanced with the use of aeration [67]. The combined liquid and gas flow has been shown to have more effect on fouling than liquid flow with higher velocity [68]. The bubble flow rate used for membrane filtration could provide oxygen to the biomass, maintain the solids suspension, and reduce the rate of the membrane fouling [69]. The objective of this current research is to investigate the performance of mixed matrix membrane in treating wastewater of palm oil mill effluent toward the different morphologies of used membrane based on varied air gap differences of 0, 3, and 5 cm. Moreover, the use of aeration was also studied on the size and velocities of bubbles. Herein, in this work, polivinylidene fluoride (PVDF), an inexpensive hydrophobic polymer, was chosen as a polymer for preparing PVDF-MMM through a non–solvent-induced phase inversion technique. This research also investigated the effect of suspended solids concentration, air bubbles flowrate (2.0, 3.0, and 4.0 mL min^{-1}), and size of bubble generation (4 and 8.5 μm) on flux and suspended solids removal.

The membrane is a promising method to be used in POME treatment due to its high packing density and the ease of module manufacture and operation. In this device, membranes are directly immersed in the feed reservoir with the withdrawal of permeate through the fibers by the application of vacuum on the outlet of the fiber lumen [70]. According to the reports, palm oil industry wastewater was characterized

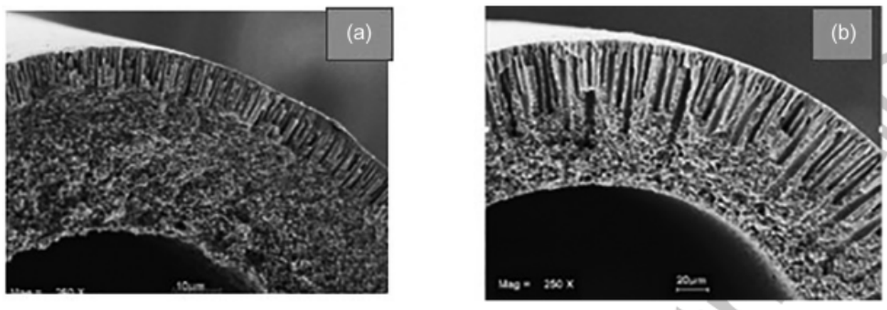

FIGURE 11.12 Cross-section image of PVDF membrane (a) without TiO_2 and (b) with TiO_2 4 wt.%.

by the presence of several organic and inorganic substances, namely, oil and grease, chemical oxygen demand (COD), total organic carbon (TOC), sulfide, free chlorine, ammonia nitrogen, and total suspended solids (TSS) [71]. The PVDF MMMs were produced by adding inorganic TiO_2 of 4 wt.% to the dope solution. TiO_2 concentration changed the membrane structure from sponge-like to finger-like, which significantly increased the water flux. It was caused by characteristic changing from hydrophobic to hydrophilic as shown in Figure 11.12.

The process efficiency in the membrane filtration is generally affected by many factors such as aeration flow rate, mixed liquor suspended solid (MLSS) concentration, pH, and hydraulic retention time (HRT). The optimization of these variables may significantly increase the process efficiency and the practicality of MLSS concentration. HRT, pH, and air bubble flow rate (ABFR) were considered as variables, while flux, total suspended solids (TSS), and ammonia nitrogen (NH_3-H) removal efficiencies were considered as parameters that have to be maximized due to the environmental regulation.

The properties of PVDF/TiO_2 mixed matrix membranes used in this work have been described in detail in the previous study[40,72]. As a semi-crystalline polymer, PVDF generally exhibits more complicated phase separation behavior than amorphous polymer. TiO_2 was added to the spinning dope to improve thermodynamic/kinetic relations during the phase inversion process in the preparation of PVDF-based membranes, to increase the surface hydrophilicity, and thus improve membrane water productivity [72]. The lab-scale experimental set-up shown in Figure 11.13 was used in this work. The membrane separation system consisted of a feed reservoir of 12 L volume, hollow fiber bundles, a peristaltic pump, a permeate flowmeter, and an permeate collector.

The filtration experiments were conducted at room temperature and under vacuum on the permeate side (0.5 bar abs) created using a peristaltic pump (Master flex model 7553-79, Cole Palmer) with the permeate being withdrawn from the open end of fibers and constant transmembrane pressure (TMP) of 0.5 bar was maintained to let water permeate from outside to the inside of the hollow fiber. The continuous aeration produced a turbulent flow which could decrease the cake layer thickness and the average particle size.

The permeation flux and rejection of modified PVDF (Merck) membranes with adding organic additive of rutile TiO_2 in varied concentrations (2 and 4 wt.%) and

FIGURE 11.13 Membrane system.

dimethyl acetamide (DMAc, Merck) as a solvent for graywater were resulted by ultrafiltration experimental equipment as shown in Figure 11.13. Prepared modified module membrane with compositions of PVDF of 18 wt.% and titanium dioxide of 2–4 wt.% was submerged in the membrane reservoir. The suspension in a membrane reservoir with a volume of 9 L has been prepared with varying compositions of suspended solid within 3.0–6.0 mg L^{-1}. A cross-flow stream was produced by air bubbling generated by a diffuser situated underneath the membrane module for mechanical cleaning of the membrane module. The air bubbling flow rates per unit projection membrane area were set at 1.2–3.0 mL min^{-1} in order to produce proper turbulence. The filtration pressure was supplied by a vacuum pump and controlled by a needle valve and hydraulic retention time was set up at 180–240 minutes. Bubble size generation was adjusted with difference aerators that have a diameter of around 500 nm in order to have turbulence flow. Finally, permeate flow rates were continually recorded using flow meters, respectively.

11.3.2.1 Analytical Methods

The morphology of modified PVDF/TiO_2 MMMSs was analyzed using field emission scanning electron microscopy (FESEM; S-800M, Hitachi High Technology Co. Ltd., Tokyo, Japan). In order to observe the membrane cross-sections, membranes were first frozen in liquid nitrogen and then submitted to fracture. All samples of cross-sections were sputter-coated with a thin gold film prior to FESEM observation at a magnification of 8k.

11.3.2.2 Flux

Pure water permeation flux (J) was measured at reduced pressure (0.5 bar absolute) on the permeate side. Then, the flux (J) was calculated as follows:

$$J = \frac{Q}{A \cdot \Delta t} \tag{11.1}$$

where J is the flux (l/m^{2}h), V is the permeate volume (l), A is the membrane surface area (m^2), and t is the time (h).

11.3.2.3 Rejection Rate

The rejection rate was calculated according to the following equation:

$$R\% = \left(1 - \frac{C_p}{C_f}\right) \times 100 \tag{11.2}$$

where C_p and C_f are concentrations of permeate and feed solutions, respectively.

11.3.2.4 Total Suspended Solids and Ammonium Nitrogen Removal

Membrane performance of total suspended solids (TSS) and ammonium nitrogen (NH_3-N) concentrations were measured using a spectrophotometer (DR 5000, HACH) in accordance with the standard procedures of method 8006 (Photometric method) and method HR TNT 10031 (salicylate method), respectively. During the operation with high organic loading rates, the concentrations were evaluated daily and sampling was carried out three times a week. The TSS and NH_3-N removal efficiencies were calculated by Equations 11.3 and 11.4.

$$TSS\ removal\ (\%) = \frac{TSS_0 - TSS}{TSS_0} \times 100 \tag{11.3}$$

where TSSo and TSS are the initial TSS concentration of the feed synthetic greywater and permeate, respectively.

$$NH_3 - N\ removal\ (\%) = \frac{NH_3 - N_0 - NH_3 - N}{NH_3 - N_0} \times 100 \tag{11.4}$$

where NH_3-No and NH_3-N are the initial NH_3-N concentration of the feed graywater and permeate, respectively.

11.3.2.5 Morphology and Structural of Membrane

Field emission scanning electromagnetic microscopy (FESEM) of the modified membranes that has composition of PVDF of 18 wt.% and TiO_2 of 2 and 4 wt.% has the improvement of membrane morphology (Figure 11.13). It was observed that for addition of a small amount of TiO_2 nanoparticles the membrane tends to have a finger-like structure more than sponge-like macrovoids. TiO_2 nanoparticles have high specific areas and hydrophilicity that affect the mass transfer during the spinning process [40, 73]. The cross-sectional images for all hollow fibers consist of finger-like macrovoids extending from both the inner and outer wall of the hollow fiber, and an intermediate sponge-like layer. The thickness of the sponge-like layer decreases initially with an increase in TiO_2 concentration of 2–4 wt.% of the PVDF of 18 wt.% (Figure 11.14).

Based on Figure 11.14a and b, it can be assumed that there is a decreasing rejection rate (Table 11.5) with an increasing pore size of the outer surface leading to the increase in the air gap distance. This indicates that the solute transport may be governed by the pore size and pore size distribution of the external surfaces of the

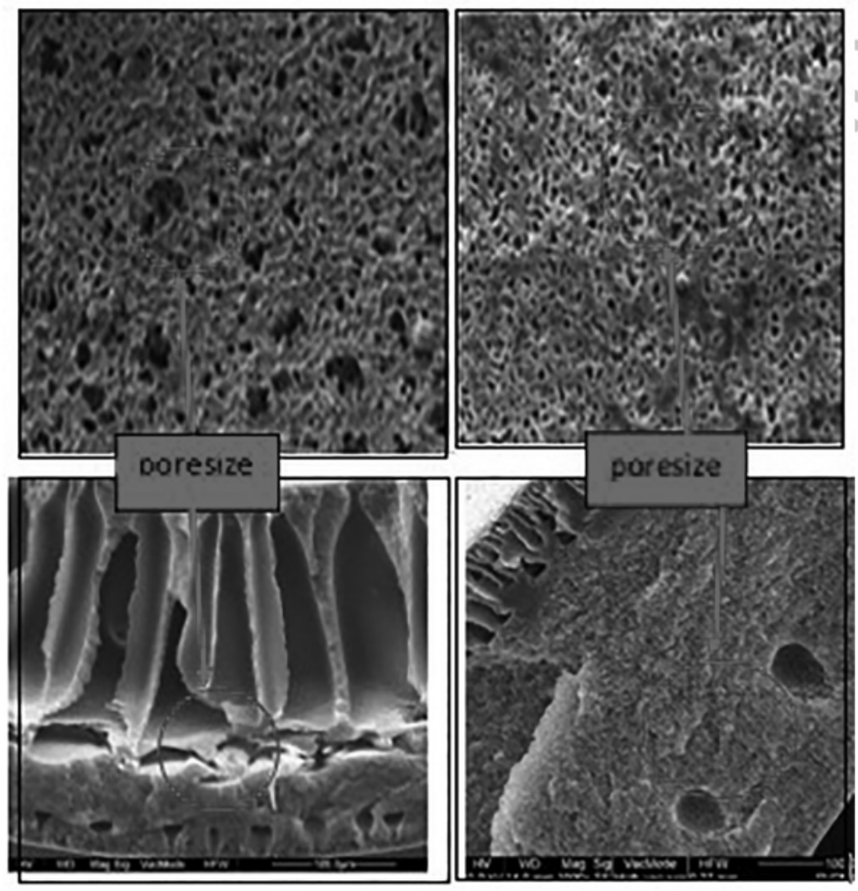

FIGURE 11.14 FESEM images of cross section of PVDF MMMs (a) with adding TiO_2 2 wt.% and (b) with adding TiO_2 4 wt.%.

TABLE 11.5
Structural and Morphology of PVDF/TiO_2 Mixed Matrix Membranes

Sample	Fluks, L/m².h	Avg poresize, nm	Porosity,%	Rejection Rate, %
PVDF		28.4		
PVDF+TiO_2 2 wt.%	30.00	10.00	65	80.25
PVDF+TiO_2 4 wt.%	87.50	38.20	86	98.90

membranes. In previous studies, it was found that lower solute separation values for hollow-MMMs have larger pore sizes [71–73]. These images showed that the membrane always used dimethyl acetamide (DMAc) as organic solvent. This solvent will change the structure of the membrane in wet conditions. The microstructural images of membranes used for liquid filtration normally performed under dry conditions. It can be proven that the structure of the membrane changes by adding the TiO_2 concentration of 2–4 wt.% where the pore size tends to be shorter and the diameter decreases. This phenomenon has been caused by swelling. This means that the microstructure images of the dry membrane could be changed significantly in wet condition, which is in the wet solvent that is trapped in membranes. These also illustrated the changes in average pore size in the membrane's outer surface with addition of TiO_2 concentration. Dzinun et al. (2020) studied mixed matrix membranes made from polyamide and reported that TiO_2 could induce an aggregate phenomenon and be absorbed into the substructure of PVDF membrane [73]. Yuliwati et al. (2011) also studied the effect of organic additives on membrane structure [40]. TiO_2 blocked the pores and caused a decrease in the average pore size of the membrane surface. The results were attributed to the porous structure and have correlated to average pore size, and porosity affecting permeate rate.

Table 11.5 shows the flux values of the used membrane containing TiO_2 of 4 wt.%. The porosity and average pore size information of the modified membrane are also tabulated in Table 11.5. All modified membranes possessed good porosity in the range of 65%–86%, which can be attributed to low polymer concentration in the membrane dope solution. The solubility of polymer and additives in the solvent plays a big role due to production of homogenous solutions before the fabrication of the hollow mixed matrix membranes. High porosity has been provided by addition of TiO_2 of 4 wt.% meaning the interaction and extrusion of TiO_2 in the porous structure and the aggregation of TiO_2 particles inside the pores. Vanneste et al. (2014) reported the interaction among active TiO_2 photocatalytic membranes [74]. They reported the possible influence of TiO_2 on the porosity of membranes. The small portion of TiO_2 in membrane dope solution could affect the interfacial stresses between polymer and TiO_2 particles. This would affect the formed pores of the organic phase during the remixing process.

The flux also increased with the increase in the concentration of TiO_2 from 2 to 4 wt.%. Table 11.5 demonstrates that the size of the average pore on the surface membrane is influenced by the value of flux.

11.3.2.6 Total Suspended Solids Removal

It can be concluded that the increase in TSS removal would occur with increasing ABFR and HRT and decreasing pH and MLSS concentrations. However, a further increase in ABFR resulted in a decrease in TSS removal. The ABFR increased from 1.2 to 2.1 ml min^{-1}, and TSS removal increased with an increase in ABFR because concentration polarization was reduced due to forceful turbulence. However, excessive aeration can cause size reduction of depositing particles due to shear-induced diffusion and inertial lift forces resulting in more severe pore blockage. Thus, there is a critical value beyond the increase of ABFR that has virtually no effect on the fouling resistance. Moreover, it could have a detrimental effect [71–73]. The turbulent

flow may consume transmembrane pressure of the system, causing weaker hydraulic and attachability factors that lead to the decline of the suspended solids removal [74].

The TSS removal was highly dependent on the pH of the feed solution. The TSS removal under various pH values was affected not only by the characteristics of the membrane but also by the properties of the solute (droplet). The size of the emulsion droplet was not uniform, and the micelles carried charges due to the reaction of surfactants. At a low pH level, the contribution of the charge neutralization predominated for micro-floc formation of relatively large sizes that were sufficient for steric hindrance. This is consistent with the conclusion made by Dzinun et al. [75]. Hence, despite the coagulated suspension that accumulated densely in the form of a cake layer at the membrane surface, the extent of suspended solid rejection was improved. The increase in suspended solid aggregation and in turn TSS removal reduction was caused by the formation of a thicker suspended solid deposit. This is likely due to the reduction of electrostatic repulsion.

11.3.2.7 Ammonium Nitrogen Removal

NH_3-N removal increased with an increase in ABFR from 1.0 to 2.5 mL min^{-1}, and then decreased with a further increase in ABFR at pH 8.00. The reason for the presence of a critical ABFR value has already been given while discussing its effect on TSS removal. ABFR must be carefully controlled to maintain adequate expansion and liquid–liquid mass transfer while minimizing shear effects. Lai et al. (2018) also mentioned that the smaller particle size in aerated submerged ultrafiltration was mainly due to the violent turbulence that aeration produced under membrane bundles [74].

It can also be concluded that NH_3-N removal increased with an increase in HRT and pH and a decrease in MLSS concentration. ABFR must be carefully controlled to maintain adequate expansion and mass transfer while minimizing shear effects near the optimum value. Lower NH_3-N removal at high MLSS concentration is due to serious membrane fouling such as membrane adsorption and pore plugging that occurs on the membrane surface. The concentration polarization on the membrane surface was also one of the factors, as has been observed at low ABFR [75]. It should however be noted that there are other reasons for the high NH_3-N removal observed. The nitrogen compounds are adsorbed to the deposited matters that are retained by the membrane in the filtration process. Besides, the biomass also assimilates organic nitrogen. This high removal value was also possible due to nitrification reactions that occurred in the reservoir where ammonium was highly soluble in water. The ammonium ions formed can be readily reduced to nitrite and nitrate. The optimal process parameters in suspended solids and ammonia nitrogen removal from palm oil wastewater were very challenging.

11.4 FUTURE CHALLENGES

Recently, novel MMMs have attracted great attention in membrane technology, due to their excellent advantages, such as some improvement in several parameters like permeability, selectivity, thermal and chemical stability, and mechanical strength of a polymeric membrane. Furthermore, the recent development demonstrated that

gas separation, as well as water treatment, has obtained significant benefit from membrane technology advancements enabling its further application in wider real industrial aspects. However, a comprehensive understanding of organic–inorganic interfaces is in a great need. MMMs performance suffers from defects caused by poor contact at the molecular sieve/polymer interface, the complexity of the synthesis process, high cost, identification of compatible inorganic particles, agglomeration, zeolite, and its applications, inorganic particle concentration, phase separation, control of morphology, and structural defects. Moreover, some MMMs for water purification application are considered to be of the potential hazard to humans and environment, and also need more research to determine the hazardous character of these nanoparticles and the mechanism of nanoparticles embedded membrane fouling in industrially water purification in the future.

One of the many difficulties associated with membrane technology is the fouling phenomenon. Although several strategies such as the incorporation of antifouling nanoparticles, and surface modification have been used to overcome this problem, intensive investigations are needed to stop the regeneration of microbial colonies on the membrane surface and to reduce the leaching of filler. The next generation MMMs should be developed by producing nano-size fillers without aggregation to improve their separation properties for the membrane industry, especially MMMs. There are several reasons to produce nano-size fillers, especially zeolite fillers such as more polymer/particle interfacial area and enhanced polymer–filler interface contact by smaller particles. The potential of incorporating fillers such as titanium dioxide particles has not been attained up to the expectation of MMMs performance, due to the smaller sizes, homogeneous distribution, agglomeration, price, availability, compatibility with polymer interface, their relationship with water chemistry, better interfacial contact, and stability.

There are limitations to developing novel materials due to costly synthesis processes. The molecular dynamic simulations (MD) of mixed matrix materials could be an effective approach to predicting the diffusive performance of MMM, especially zeolite MMMs, and to provide experimental guidelines for tuning the membrane permeability at the molecular level without high costs. Although there are previously predicted models for predicting the processes contributing to membrane separations, however, studies in MMMs showed inadequate suitable models. Therefore, MD will be essential and effective to predict the morphology and intrinsic properties of these fillers and their interaction with the polymeric matrix.

Ultimately, membrane morphology could change the properties of membranes, and subsequently, it will influence the membrane performance. Therefore, improving membrane performance in real conditions such as high temperature, high pressure, and incorporating a plasticizer into the polymer solution would be possible and essential in order to provide better thermally and chemically MMMs at different operating conditions for sustainable engineering.

11.5 CONCLUSIONS

Mixed matrix membranes with zeolite fillers have attracted a lot of attention in membrane technology research due to their excellent advantages, such as high

permeability and improved selectivity. Zeolite MMMs could be considered an ideal candidate for the purification industry since they combine the properties of polymeric matric and zeolite inorganic fillers. The application and fabrication techniques of zeolite-reinforced polymeric membranes have been comprehensively reviewed in this chapter to optimize interfacial interaction between the zeolite and the polymeric matrix. Compatibility between zeolite and polymer matrix can be improved with several methods, such as by applying high processing temperature during membrane formation, the silane modification, and priming on the particle's surface, annealing that can relax the stress imposed on hollow fiber and result in higher packing density of polymer chains, and the introduction of an LMWA agent between the polymer matrix and inorganic particles. There have been numerous implementations to incorporate zeolite particles in polymer matrices in water purification applications and for gas separation due to its superior separation properties and size exclusion. Applications of zeolite MMMs were re-evaluated for a variety of industrial processes, including water purification, medical industry, catalytic, and gas separation.

However, despite its advantages, there are still issues and difficulties associated with zeolite MMMs that have restricted their wider applications. It can be concluded that the advancements in the application and fabrication of zeolite MMM need further intensive investigations. Future research should be conducted to develop new techniques that provide a better understanding of zeolite incorporation into polymer structures. New materials should also be considered as a way of reducing fouling concerns. Additional study is necessary for an improved understanding of the basic transport mechanism occurring through the MMMs. The next generation MMMs must be developed with nano-size fillers and without aggregation to improve their separation properties severely needed in the membrane industry. Some results indicate that the nanosized zeolite particles incorporated in MMMs offer better performance in comparison with micron size particles. New additives and modification agents should be produced to improve adhesion between polymer and inorganic fillers. In conclusion, despite all the identified problems, MMM technology with zeolites could be considered a strong candidate for the modern purification industry due to the remarkable properties of polymeric and inorganic zeolite materials.

REFERENCES

1. Bokhary A., Tikka A., Leitch M., Liao B. 2018. Membrane fouling prevention and control strategies in pulp and paper industry application: A review. *J. Membr. Sci. Res.*, 4, 181–197.
2. Andrade L.H., Mendes F.D.S., Espindola J.C., Amaral M.S.C. 2014. Nanofiltration as tertiary treatment for the reuse of dairy wastewater treated by membrane bioreactor. *Sep. and Purif. Technol.*, 126, 21–29.
3. Delcolle R., Gimenes M.L., Fortulan C.A., Moreira W.M., Martins N.D., Pereira N.C. 2017. A comparison between coagulation and ultrafiltration processes for biodiesel wastewater treatment. *Chem. Eng. Trans.*, 57, 271–276.
4. Boutin O., Rowland D.J., Carpenter. 2016. Evaluating trivalent chromium toxicity on wild terrestrial and wetland plants. *Chemosphere*, 162, 355–366.
5. Eternadi H., Qazvini H. 2020. Investigation of alumina nanoparticles role on the critical flux and performance of polyvinyl chloride membrane in a submerged membrane system for the removal of humic acid. *Poly. Bull.* doi:10.1007/s00289-020-03234-z.

6. Firdayati M., Indiyani A., Prihandrijanti M., Otterpohl R. 2015. Greywater in Indonesia: Characteristic and treatment systems. *Jurnal Teknik Lingkungan*., 21(2), 98–114.
7. Frioui R, Oumeddour R., 2008. Investment and production costs of desalination plants by semi-empirical method, *Desalination*, 223, 457–463.
8. Indriani T., Herumurti W. 2010. Grey Water Treatment Using ABR-AF Reactor. Bachelor thesis. Surabaya: Institut Teknologi Sepuluh Nopember Surabaya.
9. Leal R.H., Temmink H. 2010. Comparison of three systems for biological greywater treatment. Water J., 2, 155–169. ISSN 2073-4441. Water.
10. Herdiansyah M.I., Yuliwati E., Mahyudin, Ismail A.F. 2017. Mathematical model of optimum composition on membrane fabrication parameters for treating batik palembang wastewater. *J. Eng. Appl. Sci.*, 12(4), 797–802.
11. Khouni I., Marrot B., Amar R.B. 2010. Decolourization of the reconstituted dye bath effluent by commercial laccase treatment: Optimization through response surface methodology. *Chem. Eng. J.*, 156, 121–133.
12. Ptel R., Park J.T., Hong H.P., Kim J.H., Min B.R. 2011. Use the block copolymer as compatibilizer in polyimide/zeolite composite membranes. *Poly. Adv. Tech.*, 22(5), 768–722.
13. Chen L.C., Huang C.M., Hsiao M.C., Tsai F.R. 2010. Mixture design optimization of the composition of S, C, SnO_2-codoped TiO_2 for degradation of phenol under visible light. *Chem. Eng. J.*, 165, 482–489.
14. Lai G.S., Yusob M.H., Lau W.J., Gohari R.J., Emadzadeh D., Ismail A.F. 2017. Novel mixed matrix membranes incorporated with dual-nanofillers for enhanced oil-water separation. *Sep. Purif. Technol*., 178, 113–121.
15. Hebbar R.S., Isloor A.M., Inamuddin, Asiri A.M. 2017. Carbon nanotube-and graphene-based advanced membrane materials for desalination. *Environ. Chem. Lett.*, 15(6430), 643–671.
16. Liao Z.L, Chen H, Zhu B.R, Li H.Z. 2015. Combination of powdered activated carbon and powdered zeolite for enhancing ammonium removal in micro-polluted raw water. *Chemosphere*, 134, 127–132.
17. Daraei P., Madaeni S.S., Ghaemi N., Ahmadi Monfared H., Khavidi M.A. 2013. Fabrication of PES nanofiltration membrane by simultaneous use of multi-walled carbon nanotube and surface graft polymerization method: Comparison of MWCNT and PAA modified MXCNT. *Sep. Purif. Technol.*, 104, 32–44.
18. Kobya M., Demirbas E., Bayramoglu M., Sensoy M.T. 2010. Optimization of electrocoagulation process for the treatment of metal cutting wastewaters with response surface methodology. *Water Air Soil Poll*., 215, 399–410.
19. Li Y., Su Y, Dong Y., Zhao X., Jiang Z., Zhang R., Zhao J., 2014. Separation performance of thin film composite nanofiltration membrane through interfacial polymerization using different amine monomers. *Desalination*, 333, 59–65.
20. Madaria P.R., Nagarajan M., Rajapagol C., Garg B.S. 2005. Removal of chromium from aqueous solutions treatment with carbon aerogel electrodes using response surface methodology. *Ind. Eng. Chem. Res.*, 44, 6549–6559.
21. Malisie, A. 2008. Sustainability assessment on sanitation system for low income urban areas in Indonesia. Dissertation for Doctoral Degree. Hamburg, Germany: TUHH.
22. Maghami M., Abdelrasoul A. 2018. Zeolite mixed matrix membranes (Zeolite-MMMs) sor sustainable engineering. Chapter 7 Interchopen.
23. Misdan N., Lau W.J., Ismail A.F., Matsuura T. 2013. Formation of thin film composite nanofiltration membrane: Effect of polysulfone substrate characteristics. *Desalination*, 329, 9–18.
24. Ahmad A.A., Abdulkarim A.A., Ismail S., Seng O.B. 2016. Optimization of PES/ZnO mixed matrix membrane preparation using response surface methodology for humid acid removal. *Korean J. Chem. Eng.*, 33(3), 997–1007.

25. Yuliwati E., Ismail A.F., Matsuura T., Kassim M.A., Abdullah M.S. 2011. Effect of modified PVDF hollow fiber submerged ultrafiltration membrane for refinery wastewater treatment. *Desalination*, 283, 214–220.
26. Qadir D., Mukhtar H., Keong L.K. 2017. Mixed matrix membranes for water purification applications. *Sep. Purif. Rev.*, 46, 62–80.
27. Mohammad A.W., Teow Y.H., Ang W.L, Chung Y.T., Oatley-Radcliffe D.L., Hilal N. 2015. Nanofiltration membranes review: Recent advances and future prospects, *Desalination*, 356, 226–254.
28. Celik E., Par H., Choi H. 2011. Carbon nanotube blended polyethersulfone membranes for fouling control in water treatment. *Water Res.*, 45, 274–280.
29. Vatanpour V., Madaeni S.S., Moradian R., Zinadini S., Astinchap B. 2012. Novel antibifouling nanofiltration polyethersulfone membrane fabricated from embedding TiO_2 coated multi-walled carbon nanotubes. *Sep. Purif. Technol.*, 90, 211–221.
30. Moustakes N.G., Katsaros F.K., Kontos A.G., Ramanos G. E., Dionysiou D.D., Falaras P. 2014. Visible light active TiO_2 photocatalytic filtration membranes with improved permeability and low energy consumption. *Catal. Today*, 224, 56–69.
31. Lau W.J., Ismail A.F. 2009. Polymeric nanofiltration membranes for textile dye wastewater treatment: Preparation, performance evaluation, transport modelling, and fouling control- a review, *Desalination*, 245, 321–348.
32. Lau W.J., Ismail A.F. 2010. Application of response surface methodology in PES/SPEEK blend NF membrane for dyeing solution treatment. *Membr. Water Treat.*, 1, 49–60.
33. Goh P.S., Ismail A.F., Hilal N. 2016. Nano-enabled membranes technology: Sustainable and revolutionary solution for membrane desalination? *Desalination*, 380, 100–104.
34. Goh P.S, Ismail F. 2014. Review: Is interplay between nanomaterial and membrane technology the way forward for desalination? *J. Chem. Technol. Biotechnol.*, 99, 971–980.
35. Pressdee J.R., Veerapaneni S., Shorne-Darby H.L., Clement J.A., Van der Hoek J.P. 2006. Integration of membrane filtration into water treatment systems, American Water Works Association (AWWA) research foundation, USA.
36. Silva E.M., Rogez H., Larondelle Y. 2007. Optimization of extraction of phenolics from Inga edulis leaves using response surface methodology. *Sep. Purif. Technol.*, 55, 381–387.
37. Vanneste J. Peumans W.J., Van Damme E.J.M., Darvishmanesh S., Bernaderts K., Geuns J.M.C., Van der Bruggen, B. 2014. Novel natural and biomimetic ligands to enhance selectivity of membrane processes for solute–solute separations: Beyond nature's logistic legacy. *J. Chem. Tech. Biotech.*, 89, 354–371.
38. Langhendries G., Baron G.V. 1998. Mass transfer in composite polymer-zeolite catalytic membranes. *J. Membr. Sci.*, 141, 265–275.
39. Khin M.M., Nair A.S., Babu V.J., Murugan R., Ramakrishna S. 2012. A review on nanomaterials for environmental remediation. *Energy Environ. Sci.*, 5, 8075–8109.
40. Drioli E, Giorno L. 2010. *Comprehensive Membrane Science and Engineering*, Elsevier, Amsterdam, Netherland.
41. Yuliwati E., Mohruni A.S., Mataram A. 2018. Green technology contribution in development of coolant wastewater filtration. *Sriwijaya. J. Env.*, 3(2), 74–79.
42. Yuliwati E., Porawati, H., Elfidiah, Melani, A. 2019. Performance of composite membrane for palmoil wastewater treatment. *J. Appl. Memb. Sci. Yech.*, 23(2), 1–10.
43. Zhu J., Tian M., Zhang Y., Zhang H., Liu J. 2015. Fabrication of a novel "loose" nanofiltration membrane by facile blending with Chitosan-Montmorillonite nanosheets for dyes purification. *Chem. Eng. J.*, 265, 184–193.
44. Wang R., Jiang X., He A., Xiang T., Zhao C. 2015. An in situ crosslinking approach towards chitosan-based semi IPN hybrid particles for versatile adsorption of toxin. *RSC Adv.*, 5, 51631–51641.

45. Chung T.S., Jiang L.Y., Li Y., Kulprathipanja S. 2007. Mixed matrix membranes (MMMs) comprising organic polymers with dispersed inorganic fillers for gas separation. *Prog. Polym. Sci.*, 32, 483–507.
46. Zhao Q., Hou J., Shen J., Liu J., Zhang Y. 2015. Long-lasting antibacterial behavior of a novel mixed matrix water purification membrane. *J. Mat. Chem. A.*, 3, 18696–18705.
47. Teli S.B., Molina S., Calvo E.G., Lozano A.E., de Abajo J. 2012. Preparation, characterization and antifouling property of polyethersulfone-PANI/PMA ultrafiltration membranes. *Desalination*, 299, 113–122.
48. Zhong P.S., Chung T.S., Jeyaseelan K., Armugam A. 2012. Aquaporin-embedded biometric membranes for nanofiltration. *J. Membr. Sci.*, 407–408, 27–33.
49. Shen Y.X., Sabo P.O., Sines I.T., Erbakan M., Kumar M. 2014. Biomimetric membranes: A review. *J.Membr. Sci.*, 454, 359–381.
50. Tang C, Wang Z, Petrinic L, Fane A.G, Halix-Nielson C. 2015. Biomimetic aquaporin membranes coming of age. *Desalination*, 368, 89–105.
51. Wang M, Wang Z, Wang X, Wang S, Ding W, Gao C. 2015. Layer-by-layer assembly of Aquaporin Z-incorporated biomimetic membranes for water purification. *Environ. Sci. Technol.*, 49, 3761–3768.
52. Theron J., Walker J.A., Cloete T.E. 2008. Nanotechnology and water treatment: Applications and emerging opportunities. *Crit. Rev. Microbiol.*, 34, 43–69.
53. Wang H., Chung T.S., Tong Y.W., Jeyaseelan K., Armugam A., Chen Z., Hong M., Meier W. 2012. Highly permeable and selective pore-spanning biomimetic membrane embedded with Aquaporin Z. *Small*, 8, 1185–1190.
54. Li X., Wang R., Tang C., Vararattanavech A., Zhao Y., Torres J., Fane T. 2012. Preparation of supported lipid membranes for aquaporin Z incorporation. *Coll. Surf. B Biointerf.*, 94, 333–340.
55. Nevárez L.M., Casarrubias L.B., Canto O.S., Celzard A., Fierro V., Gómez R.I., Sánchez G.G. 2011. Biopolymers-based nanocomposites: Membranes from propionated lignin and cellulose for water purification. *Carbohydrate Poly.*, 86(2), 732–741.
56. Tesh S.J., Scott T. 2014. Nano-composites for water remediation: A Review. *Adv. Mat.*, 26, 6056–6068.
57. Mahmoudi E., Ng L.Y., Ba-abbad M.M., Mohmmad W. 2015. Novel nanohybrid polysulfone membrane embedded with silver nanoparticles on graphene oxide nanoplates. *Chem. Eng. J.*, 277, 1–10.
58. Saf A.O., Akin I., Zor E., Bingol H. 2015. Preparation of a novel PSf membrane containing rGO/PTh and its physical properties and membrane performance. *RSC Adv.*, 5, 42422–42429.
59. Nasir R., Mukhtar H., Man Z., Mohshim D.F. 2013. Material advancements in fabrication of mixed matrix membranes. *Chem. Eng. Technol.*, 36, 717–727.
60. Alpatova A., Meshref M., McPhedran, K.N., Gamal El-Din M. 2015. Composite polyninylidene fluoride (PVDF) membrane impregnated with Fe_2O_3 nanoparticles and multiwalled carbon nanotube for catalytic degradation of organic contaminants. *J. Membr. Sci.*, 490, 227–235.
61. Biswas A.K., Md Islam R., Choudhury Z.S., Mostafa A., Kadir M.F. 2014. Nanotechnology based approaches in cancer therapeutics. *Adv. Nat. Sci Nanosci. Nanotechnol.*, 5, 043001–043012.
62. Essential composition and Quality Factors of Virgin Coconut Oil (SNI 7381: 2008), 2008.
63. Geise G.M., Paul D.R., Freeman B.D. 2014. Fundamental water and salt transport properties of polymeric materials. *Prog. Polym. Sci.*, 39, 1–42.
64. Mukherjee R., Sharma R., Saini P., De S. 2015. Nanostructured polyaniline incorporated ultrafiltration membrane for desalination of brackish water. *Environ. Sci. Water Res. Technol.*, 1, 893–904.

AU: Please provide complete reference for Ref. [66].

AU: Ref. [65] is cited in text, but the corresponding reference is not in reference list. Please provide complete details for Ref. [65].

65.
66. Standard Regulation of
67. Lukina A.O., Boutin C., Rowland O., Carpenter D.J. 2016. Evaluating trivalent chromium toxicity on wild terrestrial and wetland plants. *Chemosphere*, 162, 355–366.
68. Bokhary A., Tikka A., Leitch M., Liao B. 2018. Membrane fouling prevention and control strategies in pulp and paper industry application: A review. *J. Membr. Sci. Res.*, 4, 181–197.
69. Eternadi H., Qazvini H. 2020. Investigation of alumina nanoparticles role on the critical flux and performance of polyvinyl chloride membrane in a submerged membrane system for the removal of humic acid. Polymer Bulletin, Springer Verlag GmbH.
70. Moustakes N.G., Katsaros F.K., Kontos A.G., Ramanos G.E., Dionysiou D.D., Falaras P. 2014. Visible light active TiO_2 photocatalytic filtration membranes with improved permeability and low energy consumption. *Catal. Today*, 224, 56–69.
71. Fane A.G., Yeo A., Law A., Parameshwaran K., Wicaksana F., Chen V. 2005. Low pressure membrane processes- doing more with less energy. *Desalination*, 185, 159–165.
72. Razmjou A., Arifin E., Dong G., Mansouri J., Chen V. 2012. Superhydrophobic modification of TiO_2 nanocomposite PVDF membranes for applications in membrane distillation. *J. Membr. Sci.*, 415–416, 850–863.
73. Dzinun H., Ichikawa Y., Honda M., Zhang O. 2020. Efficient immobilised TiO_2 in polyvinylidene fluoride (PVDF) membrane for photocatalytic degradation of methylene blue. *J. Membr. Sci. Res.*, 6, 188–195.
74. Lai G.S., Lau W.J., Goh P.S., Ismail A.F., Tan Y.H., Chong C.Y. 2018. Tailor-made thin film nanocomposite membrane incorporated with graphene oxide using novel interfacial polymerization technique for enhanced water separation. *Chem. Eng J.*, 344, 524–534.
75. Vanneste J., Peumans W.J., Van Damme E.J.M., Darvishmanesh S., Bernaderts K., Geuns J.M.C., Van der Bruggen B. 2014. Novel natural and biomimetic ligands to enhance selectivity of membrane processes for solute–solute separations: Beyond nature's logistic legacy. *J. Chem. Tech. Biotech.*, 89, 354–371.

6_Taylor_and_francis_2023.pdf

ORIGINALITY REPORT

9%	9%	4%	6%
SIMILARITY INDEX	INTERNET SOURCES	PUBLICATIONS	STUDENT PAPERS

PRIMARY SOURCES

1	ejournal.undip.ac.id Internet Source	4%
2	ebin.pub Internet Source	3%
3	core.ac.uk Internet Source	3%

Exclude quotes	On	Exclude matches	< 3%
Exclude bibliography	On		